Effect of External Flow Mode on Nanofluid Mixed Convective Cooling Inside a Multi-Vented Cavity

ISMAIL ARROUB[1,*], AHMED BAHLAOUI[1], SOUFIANE BELHOUIDEG[1], ABDELGHANI RAJI[2], MOHAMMED HASNAOUI[3]

[1]Research Laboratory in Physics and Sciences for Engineers (LRPSI),
Polydisciplinary Faculty, Sultan Moulay Slimane University,
B. P. 592, 23000, Béni-Mellal,
MOROCCO

[2]Energy and Materials Engineering Laboratory (LGEM),
Faculty of Sciences and Technics, Sultan Moulay Slimane University,
B. P. 523, 23000, Béni-Mellal,
MOROCCO

[3]Laboratory of Fluid Mechanics and Energetics (LMFE),
Faculty of Sciences Semlalia, Cadi Ayyad University,
B.P. 2390, Marrakesh,
MOROCCO

**Corresponding Author*

Abstract: - The purpose of this paper is to study numerically laminar mixed convection in a multiple vented cavity. This enclosure is continuously heated by constant temperature from the bottom wall, while the other boundaries are presumably thermally insulated. The imposed water-Al_2O_3 nanofluid flow is injected or sucked. The Influences of various control parameters, e.g.: Reynolds number Re, from 200 to 5000, the solid volume fraction of nanoparticles, ϕ, from 0 to 7 %, and external flow mode (injection or suction) on the thermal patterns, the flow and the heat transfer within the enclosure are studied. Numerical results revealed that the presence of nanoparticles contributes to enhancement in the heat exchange and increase in the mean temperature within a cavity. Also, it was found that the heat performance and Applying the suction mode enhances the efficiency of cooling compared to the injection mode.

Key-Words: - Numerical study, mixed convection, injection, suction, nanofluid, multiple vented cavity.

Received: May 11, 2023. Revised: October 13, 2023. Accepted: December 4, 2023. Published: December 31, 2023.

1 Introduction

Because of numerous applications, mixed convection heat transfer has become a significant phenomenon in engineering systems. Enhancing the rate of heat exchange is crucial from an industrial and energy-saving standpoint system. For indication, a novel category of heat transfer fluid known as nanofluid is created by suspending nanoparticles in a base liquid like ethylene glycol or water. It is anticipated that these nanofluids will perform better in terms of heat transfer than traditional heat exchange fluids. The explanationis that the dissolved particles noticeably boost the nanofluids thermal conductivity which increases thermal transport and enhances heat transfer, [1]. Along these lines, many studies in heated enclosures have been conducted.

Several articles have been published to promote heat exchange via natural convection in the context of differentially heated cavities subjected to constant heating. The author [2], numerically studied the natural convection with H_2O-nanofluids in the inclined cavity. The findings led to the conclusion that nanoparticles in suspension significantly improve the heat exchange rate. Moreover, the minimum / (maximum) heat transfer occurs at $\theta = 90°$ / ($\theta = 30°$ or $45°$) according to Ra. In the same framework, the study [3], examined the effects of changing the nanofluid characteristics in rectangular cavities. They noted that according to

the Rayleigh number, Ra, type (Al_2O_3 or CuO), and volume fraction of the nanoparticles, the mean Nu, changed. In addition, it was discovered that Nu was more responsive to the viscosity models than the thermal conductivity models at high Ra. Recently, the author [4], investigated the characteristics of buoyancy-driven nanofluid heat transfer inside differently heated rectangular cavities. According to the study's findings, there is a particle loading that maximizes heat transfer. The same author [5], has constructed two empirical formulas assessment of dynamic viscosity and effective thermal conductivity of nanofluids. Another study related to a square enclosure with differential heating that is filled with Al_2O_3-water nanofluids is analyzed, [6]. The results appear that nanofluids display higher heat exchange rates than water. The natural convection stream of CuO-water nanofluid in inclined differently heated cavities was analyzed, [7]. It was discovered that the heat exchange efficiency was strongly based on particle diameter rather than its concentration within the base liquid. Also, the combination of aspect ratio and inclination angle affects the heat exchange and hysteresis region.

In most cases of natural convection in the cavity, heating is varied and heaters are placed in the cavity or on the side walls. When linear heating is applied, such a problem was addressed, [8]. Authors have shown that linearly increasing wall temperature has a higher heat exchange rate in comparison with linearly decreasing wall temperature. In this situation, the authors [9], displayed a numerical study utilizing Cu-water nanofluid. The existence of nanoparticles includes a clear impact with wavering behaviors for the stream and temperature areas. When the heater is used, we quote the study [10]. It has been observed that as the heater's length increases, Nu reduces. An additional digital investigation was conducted, [11]. Simulations indicate that heat exchange can be improved more effectively by expanding the number of HACs than expanding the HAC's size.

Many studies on this subject are concerned basically with applications involving forced convection. In this context, an experimental and numerical study was conducted, [12], [13] to examine the cooling achievement of forced convection with heat sink microchannel design nanofluid. The results showed that nanofluid cooled the heat sink better than water and had a superior heat exchange coefficient. In the studies, [14], [15] the same problem is examined experimentally and declared that even while the heat sink's thermal resistance dropped, scattering that dispersing nanoparticles in water significantly improved the heat exchange coefficient overall.

Many studies on mixed convection in lid-driven cavities containing nanofluids in different geometries have been conducted recently. In this case, authors [16], [17], observed that when Re increases, the effect of solid concentration diminishes. Also, they found that the particle distribution depends on Rayleigh and Richardson numbers. The problem of nanofluid mixed convection is treated, [18], in the case of the square cavity with a lid powered by a heat source and locally heated from below. They demonstrated how the rate of heat transfer drops as the volume percentage of nanoparticles increases for large Ra. Furthermore, it was discovered that the rate of heat transmission rises as the heat source moves toward the walls on the cold side. The authors [19], numerically analyzed mixed convection flow in a cavity operated by the lid and filled with nanofluid and heated by sinusoidal heating in a situation where the latter is variable. They demonstrated that, for a given Grashof number, the rate of heat transmission rises when the volume percentage of nanoparticles increases and the Richardson number decreases. In some studies related to the geometry of square cavities with mobile lids and heating is localized inside, [20]. The results of this study showed that, when the diameter of the nanoparticles increases, a reduction of Nu for all Ri is observed.

Relatively little study has been done in the past few decades on mixed convection for nanofluids in vented cavities with constant heat flux or temperature. This kind of issue is crucial for many different kinds of technology applications. Therefore, the authors [21], carried out a numerical analysis of the situation with applying uniform heat flow. The rate of heat transfers at the heat source area increased and average bulk temperature decreased as solid concentration increased, according to the presented results. The authors [22], reexamined the same topic for various port locations in the event of completely continuous heating. It was discovered that the Bottom-Top configuration benefits more from the addition nanoparticles than the other configurations that were taken into consideration. Nanofluid mixed convective cooling in a vented cavity locally heated on one side by a heat source, was investigated numerically, [23]. Their results showed that a full entropy production in the cavity when a heater is embedded in the bottom wall compared with others. The authors [24], carried out a numerical analysis of mixed convection across a ventilated square cavity with Al_2O_3-water nanofluid under uniformly applied

temperature. The results presented revealed that the inclusion of nanoparticles increases the Nu and value of the pressure dropping coefficient. In the case of a hot obstacle in the enclosure, [25], the study's findings showed that the heat transfer rate was increased for various Ri and outlet port placements by incorporating nanoparticles into the base fluid. The same study was examined, [26], where two hot square obstacles are situated in the cavity's bottom wall and they concluded the same remarks. The authors [27], [28], studied mixed convection heat exchange of an Al_2O_3-water nanofluid in ventilated cavities as a result of incoming and outgoing flow by application of the two modes of injection and suction for various heating purposes. In these studies, adding nanoparticles positively impacts the heat exchange, but it also increase the average temperature in the cavity.

The study of mixed convection in an enclosure that is isothermally heated and vented by multiple ports utilizing two separate modes and nanofluid has not yet been studied, according to the research currently available quoted in the literature review above. Therefore, this research is focused on studying such problems, because of many modern processes, like design for solar collectors, the thermal design constructions, cooling process for electronic circuits and heat exchangers, [29], [30], [31], [32]. Hence, the effects of key variables on flow and energy fields are investigated and analyzed. These parameters include the Reynolds number, the concentration of nanoparticles, and imposed flow (injection or suction).

2 Description of the Problem

Figure 1 displays a schematic illustration of a studied configuration. It is made up of an A = 2 rectangular horizontally vented cavity. It is assumed that all borders are thermally insulated, whereas the lower wall is heated at constant temperature. Throughout the two openings on the bottoms of the right and left vertical walls, an external nanofluid stream is forced through the cavity by injection (Figure 1a) and suction (Figure 1b), subjecting the physical system to the force. To ensure the ventilation process, a third opening is situated in the center of the upper wall. We assume that there is no slip occurring between the two phases and pure water and nanoparticles are in a condition of thermal stability.

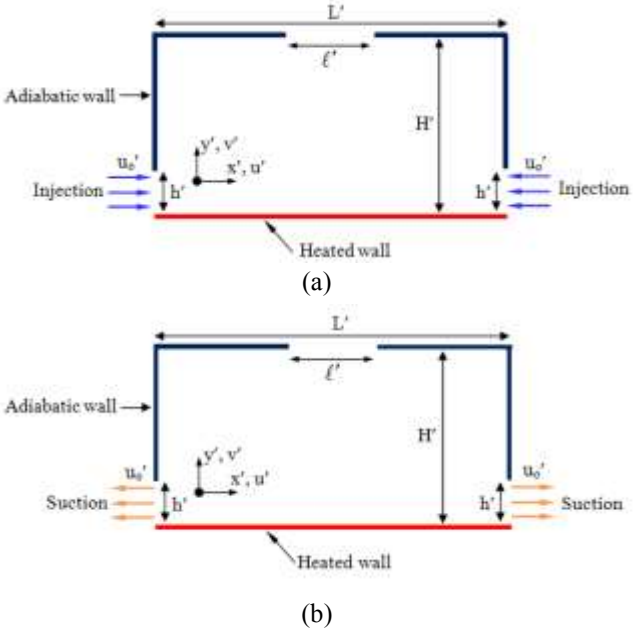

Fig. 1: The problem's geometry: a) Injection mode and b) Suction mode

As is shown in Table 1, [33], the thermophysical characteristics of the alumina nanoparticles under investigation and pure water are evaluated during average nanofluid temperature (T′ = 32°C). With the exception of density with the force of buoyancy, Boussinesq's approximation is still correct, the parameters of the nanofluid are taken to be constant. It is assumed that the flow in this investigation is laminar and two-dimensional. The nanofluid utilized is Newtonian and incompressible. Moreover, thermal radiation and viscous dissipation are not taken into consideration.

Table 1. Thermophysical characteristics of both nanoparticles and water, T′ = 32°C, [33]

	(H_2O)	(Al_2O_3)
$\rho \times 10^2$ (kg/m^3)	9.95	39.70
c_p (J/kg.K)	4178	765
λ (W/m.K)	0.62	36
$\beta \times 10^{-5}$ (K^{-1})	32.06	0.846
$\mu \times 10^{-6}$ (N.s/m^2)	769	---
ρ_{fo} (kg/m^3) at T′ = 293 K	998.29	---

3 Mathematical Modeling

The general equations governing the convection processes for Newtonian nano-fluid are obtained using the fundamental principles of conservation of energy, momentum, and mass. Solving the problem described by these conservation equations consists

of determining the various unknown quantities u′, v′, P′ and T′ involved in these equations.

Considering the hypotheses previously cited, the basic dimensionless formulas governing the movement of the nanofluid and the heat transfers in mixed convection are:

- The continuity equation:

$$\frac{\partial \mathrm{u}'}{\partial \mathrm{x}'}+\frac{\partial \mathrm{v}'}{\partial \mathrm{y}'}= 0 \tag{1}$$

- The conservation of momentum equation

● Following ox′ direction:

$$\frac{\mathrm{du}'}{\mathrm{dt}'}=-\frac{1}{\rho_{\mathrm{nf}}}\frac{\partial \mathrm{P}'}{\partial \mathrm{x}'}+\frac{1}{\rho_{\mathrm{nf}}}(\rho\beta)_{\mathrm{nf}}\, g\,(\mathrm{T}'-\mathrm{T}'_{\mathrm{R}})+\nu_{\mathrm{nf}}\left[\frac{\partial^2 \mathrm{u}'}{\partial \mathrm{x}'^2}+\frac{\partial^2 \mathrm{u}'}{\partial \mathrm{y}'^2}\right] \tag{2}$$

● Following oy′ direction:

$$\frac{\mathrm{dv}'}{\mathrm{dt}'}=-\frac{1}{\rho_{\mathrm{nf}}}\frac{\partial \mathrm{P}'}{\partial \mathrm{y}'}+\frac{1}{\rho_{\mathrm{nf}}}(\rho\beta)_{\mathrm{nf}}\, g\,(\mathrm{T}'-\mathrm{T}'_{\mathrm{R}})+\nu_{\mathrm{nf}}\left[\frac{\partial^2 \mathrm{v}'}{\partial \mathrm{x}'^2}+\frac{\partial^2 \mathrm{v}'}{\partial \mathrm{y}'^2}\right] \tag{3}$$

With P′, designates the effective pressure of the nanofluid.

- The energy conservation equation

$$\frac{\mathrm{dT}'}{\mathrm{dt}'}=\alpha_{\mathrm{nf}}\left[\frac{\partial^2 \mathrm{T}'}{\partial \mathrm{x}'^2}+\frac{\partial^2 \mathrm{T}'}{\partial \mathrm{y}'^2}\right] \tag{4}$$

Therefore, under the above-mentioned equations and using the stream function and vorticity definitions, the differential equation system that controls the transport of a nanofluid in the cavity in two dimensions may be expressed as:

$$\frac{\partial \Omega'}{\partial t'}+u'\frac{\partial \Omega'}{\partial x'}+v'\frac{\partial \Omega'}{\partial y'}=\frac{(\rho\beta)_{nf}}{\rho_{nf}}g\frac{\partial T'}{\partial x'}+\nu_{nf}\left(\frac{\partial^2 \Omega'}{\partial x'^2}+\frac{\partial^2 \Omega'}{\partial y'^2}\right) \tag{5}$$

$$\frac{\partial T'}{\partial t'}+u'\frac{\partial T'}{\partial x'}+v'\frac{\partial T'}{\partial y'}=\alpha_{nf}\left[\frac{\partial^2 T'}{\partial x'^2}+\frac{\partial^2 T'}{\partial y'^2}\right] \tag{6}$$

$$\frac{\partial^2 \Psi'}{\partial x'^2}+\frac{\partial^2 \Psi'}{\partial y'^2}=-\Omega' \tag{7}$$

For a two-dimensional flow, the following relations correlate the velocity components to the vorticity and the stream function:

$$u'=\frac{\partial \Psi'}{\partial y'} \quad ; \quad v'=-\frac{\partial \Psi'}{\partial x'} \quad , \quad \Omega'=\frac{\partial v'}{\partial x'}-\frac{\partial u'}{\partial y'} \tag{8}$$

The following correlations are the expressions for Effective density, thermal diffusivity, heat capacitance, and thermal expansion coefficient of nanofluid, in that order, [11], [34]:

$$\rho_{nf}=\phi\rho_s+(1-\phi)\rho_f \tag{9}$$

$$\alpha_{nf}=\frac{\lambda_{nf}}{(\rho c_p)_{nf}} \tag{10}$$

$$(\rho c_p)_{nf}=\phi(\rho c_p)_s+(1-\phi)(\rho c_p)_f \tag{11}$$

$$(\rho\beta)_{nf}=\phi\rho_s\,\beta_s+(1-\phi)\rho_f\beta_f \tag{12}$$

The following correlations, can be used to predict effective dynamic viscosity, μ_{nf}, and effective thermal conductivity, λ_{nf}: utilizing a vast array of data from experiments collected by various studies, [5]:

$$\lambda_{nf}=\lambda_f\left[1+4.4\ Re_s^{0.4}\,Pr^{0.66}\left(\frac{T}{T_{fr}}\right)^{10}\left(\frac{\lambda_s}{\lambda_f}\right)^{0.03}\phi^{0.66}\right] \tag{13}$$

$$\mu_{nf}=\mu_f\left[\frac{1}{1-34.87\left(d_s/d_f\right)^{-0.3}\phi^{1.03}}\right] \tag{14}$$

The strength of equations (13) and (14) were recently tested through an examination of comparison using multiple experimental databases compared to those employed in generating them. The results showed a fairly good degree of acceptance, in addition to the fact that both of them precisely approximate the results from experiments that form their basis, [35], [36].

Hence, the dimensionless variables listed below should be used:

$$A=L'/H',\ B=h'/H',\ x=x'/H',\ y=y'/H',u=u'/u'_o,$$
$$v=v'/u'_o,t=t'u'_o/H',T=(T'-T'_C)/(T'_H-T'_C),\Psi=\Psi'/u'_oH',$$
$$Re=u'_oH'/\nu_f\ \ \Omega=\Omega'H'/u'_o,Pr=\nu_f/\alpha_f\ \ Ra=g\,\beta_f(T'_H-T'_C)H'^3/\alpha_f\nu_f,.$$

The equations that govern the problem without dimensions formulation are provided by including the variables without dimensions and given as:

$$\frac{\partial \Omega}{\partial t}+u\frac{\partial \Omega}{\partial x}+v\frac{\partial \Omega}{\partial y}=\frac{Ra}{\mathrm{Re}^2\,\mathrm{Pr}}\left[\left(\frac{\phi}{(1-\phi)\frac{\rho_f}{\rho_s}+\phi}\right)\times\frac{\beta_s}{\beta_f}+\frac{1}{\left(\frac{\phi}{(1-\phi)}\frac{\rho_s}{\rho_f}+1\right)}\right]\frac{\partial T}{\partial x}+\frac{1}{\mathrm{Re}}\times\left[\frac{\frac{\mu_{nf}}{\mu_f}}{\left(\phi\frac{\rho_s}{\rho_f}+(1-\phi)\right)}\right]\left(\frac{\partial^2 \Omega}{\partial x^2}+\frac{\partial^2 \Omega}{\partial y^2}\right) \tag{15}$$

$$\frac{\partial T}{\partial t}+u\frac{\partial T}{\partial x}+v\frac{\partial T}{\partial y}=\frac{1}{Re\,Pr}\left(\frac{\frac{\lambda_{nf}}{\lambda_f}}{(1-\phi)+\phi\frac{(\rho c_p)_s}{(\rho c_p)_f}}\right)\times\left(\frac{\partial^2 T}{\partial x^2}+\frac{\partial^2 T}{\partial y^2}\right) \quad (16)$$

$$\frac{\partial^2 \Psi}{\partial x^2}+\frac{\partial^2 \Psi}{\partial y^2}=-\Omega \quad (17)$$

Here are the definitions of vorticity and the dimensionless stream function:

$$u=\frac{\partial \Psi}{\partial y}\quad ;\quad v=-\frac{\partial \Psi}{\partial x}\quad \text{and}\quad \Omega=\frac{\partial v}{\partial x}-\frac{\partial u}{\partial y} \quad (18)$$

3.1 Border Conditions

When used the two ventilation modes, the same boundary conditions in the without dimensions form are established as follows:

$u = v = 0$ no-slip flow condition for the sides
$T = 1$ and $\Psi = 0$ in the lower horizontal hot side
$\frac{\partial T}{\partial n} = 0$ in adiabatic sides

″n″ The outside perpendicular to the proposed adiabatic side

Suitable boundary conditions without dimensions about suction or injection scenarios can be expressed as:

Injection case:

$u = 1$, $T = v = \Omega = 0$, $\Psi = y$ in cavity's left entrance
$u = -1$, $T = v = \Omega = 0$, $\Psi = -y$ in cavity's right entrance
$\Psi = -B$ within the top output and the right input
$\Psi = B$ within the top output and the left input

Suction case:

$T = 0$ in a top input
$u = -1$, $v = 0$, $\Psi = -y$, $\Omega = 0$ in a left output
$u = 1$, $v = 0$, $\Psi = y$, $\Omega = 0$ in a right output
$\Psi = -B$ within a top input and a left output
$\Psi = B$ within a top input and a right output

About the vorticity, which is unknown on the solid boundary, the author, [37], found an approximation relation, was used for its stability and accuracy, such as:

$$\Omega_w=-\frac{1}{2}\Omega_{w+1}-\frac{3}{\Delta\eta^2}\left(\Psi_{w+1}-\Psi_w\right) \quad (19)$$

Is utilized because of its precision and stability, where w denotes a wall, Δη for a space step that is taken in the wall's normal orientation.

3.2 Heat Transfer Calculation

In engineering applications, the total heat transmission throughout the cavity is a crucial metric. The mean Nusselt number, Nu, along a bottom active wall is used to express it, and it is assessed as follows [38]:

$$\mathrm{Nu}=-\frac{1}{\mathrm{A}}\left(\frac{\lambda_{\mathrm{nf}}}{\lambda_{\mathrm{f}}}\right)\int_0^{\mathrm{A}}\left.\frac{\partial \mathrm{T}}{\partial \mathrm{y}}\right|_{\mathrm{y}=0}\mathrm{dx} \quad (20)$$

4 Numerical Solution Procedure

A finite difference approach was utilized to discretize equations that govern the system, which are Eqs. (15), (16) and (17), in combination with their related boundaries. A second-order central difference method approximated the diffusive terms' first and second derivatives. In addition, a second-order upwind differencing method was applied to advection terms to prevent probable instabilities that are often seen in mixed convection challenges. Temporal integration for Eqs. (15) and (16) were then carried out using an alternating direction implicit (ADI) approach. Using the point sequential over-relaxation method (PSOR) at every time step, the Poisson equation, Eq. (17), was solved. For a grid (201×101) used in this work, the optimal over-relaxation coefficient was 1.95. The agreement on convergence criteria $\sum_{i,j}\left|\Psi_{i,j}^{n+1}-\Psi_{i,j}^{n}\right| \Big/ \sum_{i,j}\left|\Psi_{i,j}^{n+1}\right| < 10^{-5}$ was met for Ψ every step, this $\Psi_{i,j}^{n}$ is the stream function result for the n^{th} execution level at node (i,j). According to the governing parameter values, a range of time stepping sizes $10^{-5} \le \delta t \le 10^{-3}$ were chosen.

5 Validation of Code and Studies on Grid Independence

In numerical modeling, computational code validation is crucial. Verifying the accuracy of this numerical code was done by contrasting our findings with numerical results reported in the study [21], of mixed convection flows in a vented square cavity filled with CuO-water nanofluid that were heated locally by a constant flux. Figure 2 displays

comparative findings for Re = 100 based on Nu assessed on the heated portion on the lower wall. When changing ϕ from 0 to 5% and Ri = 0.1, 1, and 10, the highest variances seen stay under 1.02%. Additionally, Our code was confirmed by comparing it to the experiment results of the authors [39], for natural convection in a square cavity containing an alumina-water nanofluid and heated differently for H′ × L′ = 25 mm × 25 mm, different values of Ra and ϕ = 0.1 %. Comparing findings with the highest differences of about 4.5% are shown in Table 2 and pertain to Nu assessed against the hot wall. Therefore, these findings guarantee the correctness of the current code used to investigate the considered problem.

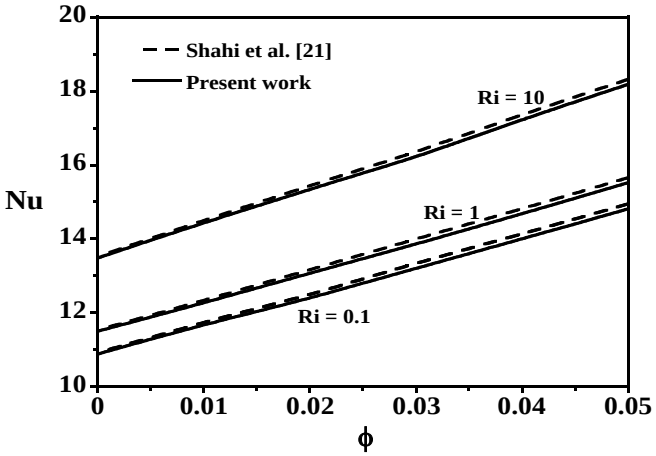

Fig. 2: Comparing Nu, for Re = 100 and various values of ϕ and Ri in vented square cavity exposed to copper-water nanofluid

Table 2. Verification of the numeric code for various values of Ra using Nu assessed on hot wall in square cavity that contains Al_2O_3 and water nanofluid

Ra	Current study	Ho et al. [39] (Experimental)	percentage of variation
$7.5\ 10^5$	7.91	7.6	4.08
$1.5\ 10^6$	9.801	9.4	4.26
$2.5\ 10^6$	11.79	11.3	4.33
$3.3\ 10^6$	12.54	12	4.5

To verify that the solution was grid-independent, a full mesh testing process was carried out. For both the x and y axes, a uniform size of grid 201×101 is employed in all calculations for this investigation. By contrasting the findings from this grid with those from a finer grid of 321×161, grid sensitivity research has been carried out (Table 3). Indeed, in terms of Ψ_{max} and Nu, the highest relative error generated is less than 1.06 percent and 1.76 percent, respectively.

Table 3. Examination results of grid independence with 1 and 2 corresponds to (201×101) and (321×161) respectively for various Re and ϕ values for the suction and the injection forced flow

		ϕ = 0.04		**ϕ = 0.07**	
		Ψ_{max}	**Nu**	**Ψ_{max}**	**Nu**
Injection flow Re=600	**1**	0.279	18.892	0.279	19.327
	2	0.281	19.191	0.281	19.665
Injection flow Re=2000	**1**	0.282	33.155	0.282	33.820
	2	0.285	33.496	0.285	34.182
Suction flow Re=200	**1**	0.297	23.987	0.297	24.423
	2	0.298	23.564	0.298	23.996
Suction flow Re=3000	**1**	0.284	96.540	0.284	98.717
	2	0.284	97.214	0.284	99.575

6 Findings and Discussions

We conduct numerical simulations to investigate the temperature and convective flow patterns in a multi-vented enclosure, heated with uniform hot temperature at the bottom horizontal wall. This simulation are performed for a Reynolds number (Re) varied between 200 and 5000 and a volume fraction of nanoparticles (ϕ) that varies from 0% to 7%, while maintaining a fixed Rayleigh number of $Ra=10^6$. The analysis evaluates the conjugate effects of Re, ϕ and the applied flow mode via the cavity on temperature distribution, cooling efficiency, and fluid flow. It will be noted that, low values of Re (Re ≤ 500) in the injection mode lead to unsteady solutions, which do not clearly show up as dynamic and thermal structures in the region of the instability zone.

Figures 3a-3d show streamlines and isotherms plots for the two cases ϕ = 0 (continuous line —) and ϕ = 0.07 (discontinuous line - - -), demonstrating the effect of Re on thermal fields and dynamical in injection mode. Four closed-cell structures are seen in the streamlines at the moderate value of Re (Re = 600) (Figure 3a). Therefore, the two cells in the highest part of the cavity on the right (clockwise cell) and left (trigonometric cell) correspond to those located above open lines of forced flow caused by shear effects. Both with heated walls, turning in opposite directions because

of shear effects and free convection. By raising ϕ from 0 to 0.07, qualitatively, a very small effect in the stream pattern can be seen. There is an adequate convective heat transfer entre the liquid and the active horizontal wall, as indicated by the matching isotherms that tighten at that level. In addition, there are two cold zones which are delimited by an inlet opening and that of the exit.

These two zones are brought eventually to a uniform temperature that is equal to that of the external environment. The presence of this characteristic attests to an absence of heat transmission via the active wall and the surrounding walls. Furthermore, because the comparable isotherms for the pure water and $\phi = 0.07$ are well spaced, the impact of ϕ is greatly noticeable where the two little bottom cells are located. As the influence of forced convection increases, an increase in Re up to 1000 (Figure 3b) causes a rise in the size as well as the intensity of the two lower cells (which are compared to the higher cells), which allows straightening of the open lines and consequently leaving enough space in favor of the two cells. Re is subsequently increased to 3000 and eventually 5000 (dominant forced convection regime) in order to support the bottom cell, as Figures 3c-3d illustrate. This improvement is to detriment of open lines which become relatively straight. However, for high numbers of Re, the thermal and dynamic structures grow insensitive to the quantity of nanoparticles. Near the heated wall, all isotherms condense, as indicated by the corresponding isotherms, by forming a distinguished and very thin thermal boundary layer. This behavior testifies an intense heat released via the open lines to the exterior either directly or through the two lower cells.

The streamlines and isotherms are also displayed in the enclosure in the suction case in Figures 4a–4e for both $\phi = 0$ (continuous line —) and $\phi = 0.07$ (discontinuous line - - -) and different Re values. As illustrated in Figure 4a, the streamlines observed at low Re values (Re = 200) demonstrate that the forced flow is sucked vertically through the opening situated in the middle of the top wall, then leaving horizontally the cavity from the two vertical outlets. Therefore, the lower hot wall is in direct contact with the horizontal and parallel open lines, which allows a strong thermal exchange of this wall and the fluid. The existence of two large, enclosed cells defines the structure with the same size and opposite senses, surmounting the promoted flow's open lines and whose formation is mostly caused by shear force compared to the larger cells that are visible on injection, such cells are straight, big, and intense (Figure 3a). In addition, the dynamic structure is symmetrical about the middle of the configuration, as demonstrated. The associated isotherms are condensed as a beam in the vicinity from the horizontal wall that is heated, which forms a thermal boundary layer of low thickness indicating a powerful convective heat transmission from the fluid's wall. As a result, the heat generated in the hot wall is immediately evacuated via thermal boundary layer to exit. Maybe said in this situation that the inertia forces dominate over the forces of buoyancy. Besides, we note that the thermally inactive zone (cold zone) occupies almost the entire cavity. This behavior indicates that the technique of suction is thermally stronger compared to the injection mode. The two enclosed cells sizes somewhat grow because of the increase of the forced flow when Re is increased up to 600 and 1000 (Figures 4b-4c).

The isotherms demonstrate a reduction of the cold zone relative to the boundary layer, indicating an increase in the impact of forced convection. An additional raise of Re up to 3000 and then 5000 does not encourage the modification of the flow structure (Figures 4d-4e) but contributes to the reduction of the thermal border layer in favor of the cold region and subsequently to the improvement of the thermal transfer. In the end, it needs to be emphasized that the existence of nanoparticles (from $\phi = 0$ to $\phi = 0.07$) does not modify the dynamic and thermal structures, whatever the intensity of the forced flow.

We used Figure 5 to demonstrate the variation between the Nu and the Re, and different values of ϕ along the wall that is heated, to show the success that modes performed during the heat removal process. Overall, Nu increase with Re in both modes. At $Re \approx 500$, the rate of this growth gains significance (beyond this threshold, an increase in the curve's slope is seen). The intensity of the flow supports this pattern that occurs as a result of the inertia forces generated by the rise in Re.

On the other hand, Nu in the injection situation is nearly constant as long as $Re < 500$. The explanation for this outcome is that, over this range of Re, natural convection predominates and therefore, for any given Re, the impact on the transmission of heat is insignificant. This result is because the appearance of two closed cells which delays the transfer of heat in the situation of low-velocity flow through the fluid and heated wall.

About the suction mode, this single point does not exist because of the imposed flow keeps the heated wall entirely in direct contact, resulting in a constant rise in Nu with Re. When ϕ is increased to 0.07, for a fixed value of Re, the convection increases noticeably in both mode conditions. This

is because as ϕ increases, the nanofluid's effective thermal conductivity also increases. More specifically, Nu is raised for the more fortunate scenario by raising ϕ from 0 to 0.07, used for Re = 5000, from 106.26 / (49.43) to 116.17 / (53.55) for the suction / (injection) case.

It should be mentioned that the difference between suction and injection, improves heat transfer more, resulting in more cavity cooling for all Re values, whether the cavity is packed with either nanofluid or water.

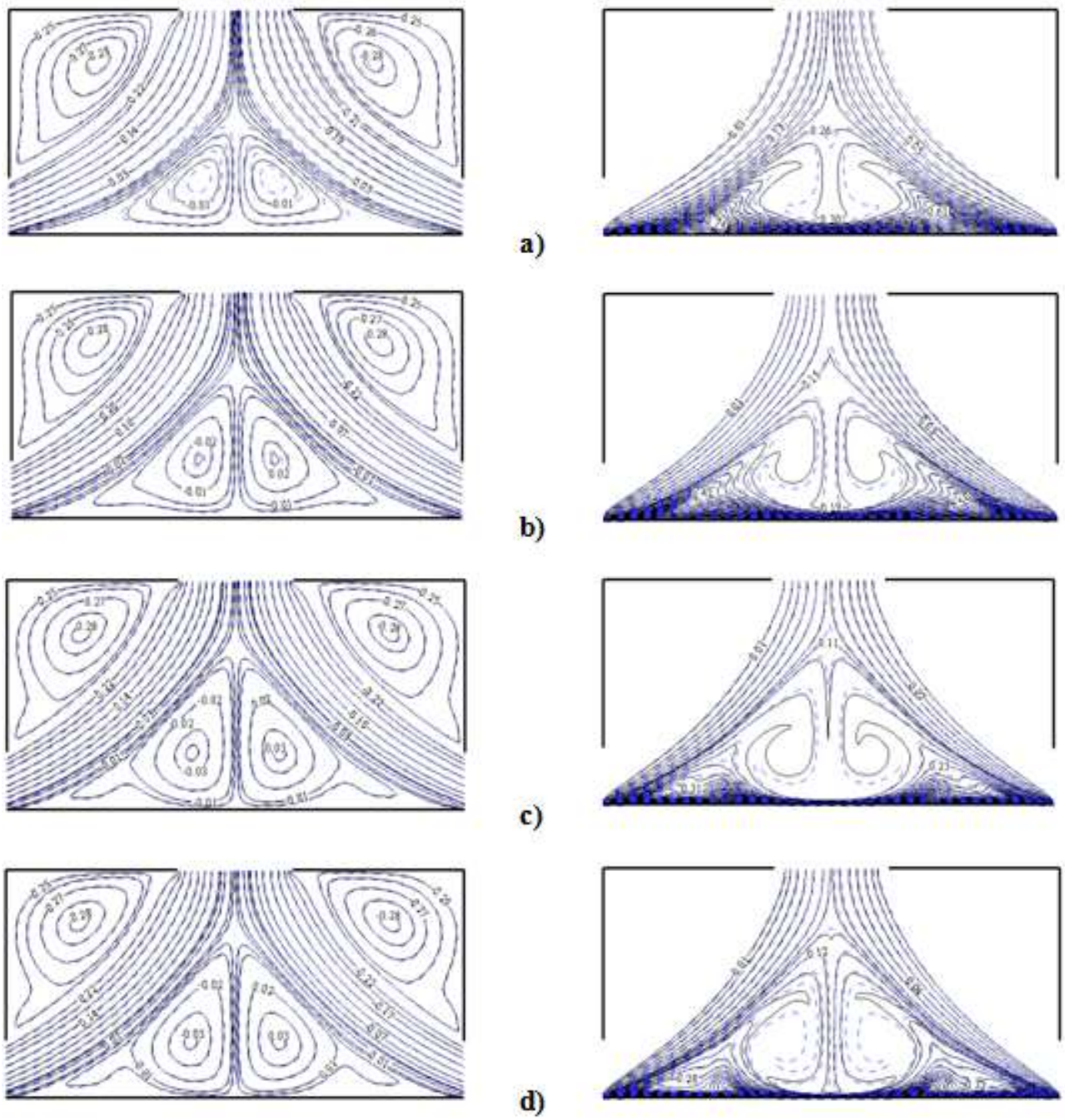

Fig. 3: Streamlines and isotherms, for ϕ = 0 (—) and ϕ = 0.07 (- - -), various values of Re, with injection case: a) Re = 600, b) Re = 1000, c) Re = 3000 and d) Re = 5000

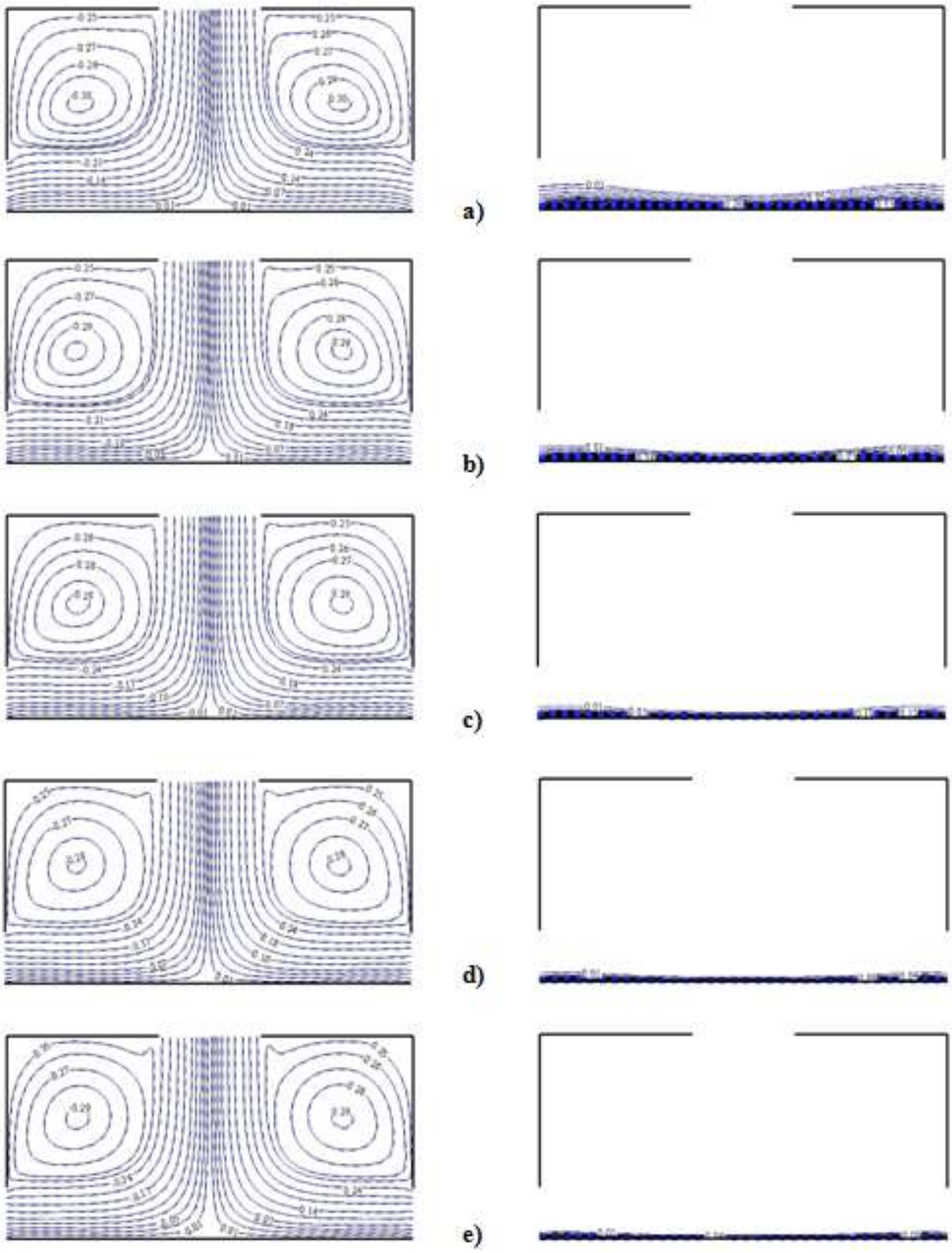

Fig. 4: Streamlines and isotherms, for $\phi = 0$ (—) and $\phi = 0.07$ (- - -), various values of Re, with suction case: a) Re = 200, b) Re = 600, c) Re = 1000, d) Re = 3000 and e) Re = 5000

Furthermore, in mixed or forced convection (moderate Re values), the suction case thermal performance is more noticeable. This revealed result proves the originality of our work since the most of earlier research examined the injection mode while examining the ventilated systems' thermal capabilities. Quantitatively, for $\phi = 0.04$ and Re = 1000 Nu rises from 23.59 to 58.23 when switching from injection to suction mode which corresponds to a multiplication of the heat transfer rate of almost 2.5.

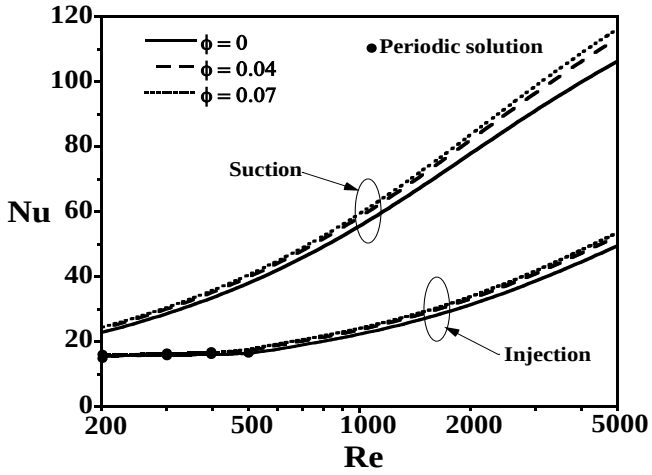

Fig. 5: Variations of Nu, with respect to Re for various values of ϕ in both injection and suction mode.

It should be emphasized that oscillatory action is frequently seen during the time of a shift from one flow to another structure to another, when the heating is applied by the bottom or when Ra is sufficiently high and Re is less than the critical value. Thus, in the mode of injection, unsteady periodic solutions have been obtained; they are marked by full circles in Figure 5. For such cases, Nu is averaged over multiple flow cycles. When Re rises over a critical value, these unstable solutions vanish. For more precision, the existence of these periodic solutions is restricted with ($200 \leq Re \leq 500$) depending on ϕ.

Figures 6a–6b provide an example of a typical periodic solution and show the unsteady periodic regime in terms of Ψ_{min} and Nu, in the injection mode, for Re = 300 and $\phi = 0.04$. The nature of the For Nu, the fluctuations are sinusoidal, although this sinusoidal behavior is lost for Ψ_{min} during a short interval. Both variables (Ψ_{min} and Nu) oscillate at identical periods in space and time. By the norm of the author [40], the analogous trajectory in the (Ψ_{min}, Nu) phase plane is a straightforward closed curve of the P_1-type.

The cycle's limits are projected in the phase plane in Figure 6c. Figure 6b shows streamlines and isotherms at specific moments that correspond to the characters ‘a’ to ‘e’ throughout one flow cycle.

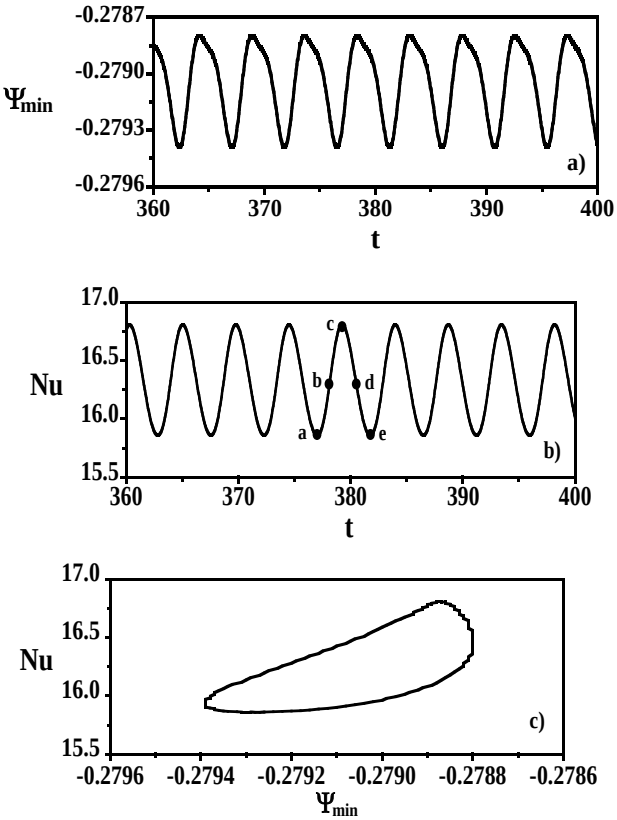

Fig. 6: Periodic oscillations, obtained for Re = 300 and $\phi = 0.04$ in the injection case: a) variations with time of Ψ_{min}, b) variations with time of Nu and c) projection at a phase plane Ψ_{min}-Nu.

Figures 7a–7e show that as the cycle evolves, there are minor changes to the temperature and flow structure within the enclosure. But it is to indicate that an alternation of appearance and disappearance of the two cells below the forced lines is marked. The existence of these convective cells is favored by natural convection's significance. This observed phenomenon is justified by the competition between natural and forced convection, which causes the appearance of an oscillatory regime. In addition, the corresponding isotherms show clearly that, there is some complication in the temperature distribution within the cavity in the lower center section. (Deformation of isotherms) because of this area’s complicated flow structure, located where two small cells are situated.

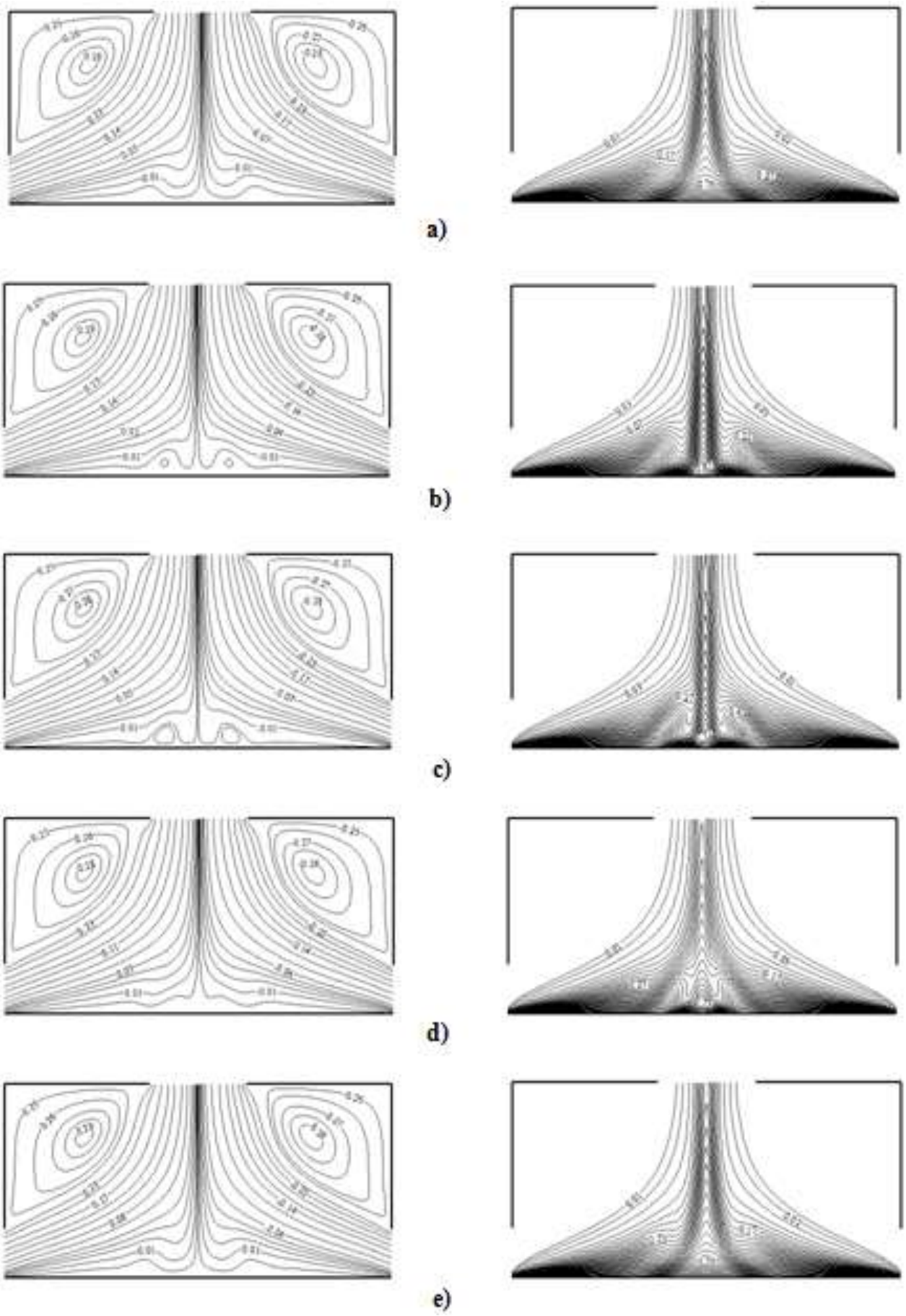

Fig. 7: Streamlines and isotherms, during one flow cycle, in injection case, for Re = 300 and $\phi = 0.04$

The improvement of the heat exchange by the suction mode's accomplishment is demonstrated in Figure 8 regarding the injection case, presents the variation with Re of the parameter $E_{mod} = [(Nu_{suction} - Nu_{injection}) / Nu_{injection}] \times 100$. For any value of ϕ, E_{mod} crosses as a monotonous way with Re up to a maximum value that corresponds to a critical Re (Re_c = 1500). Quantitatively, in the case of ϕ = 0.07, E_{mod} reaches its maximum value which is approximately 150% (ie, the amount of heat released is amplified by 2.5 times). Beyond Re_c, any increase in Re involves a drastic reduction of E_{mod}. The consequence of this analysis shows the contribution of the suction case is favored by Re as Re < 1500. On the other hand, for a given Re, we deduce that, the contribution of the suction case is supported by ϕ for Re < 500.

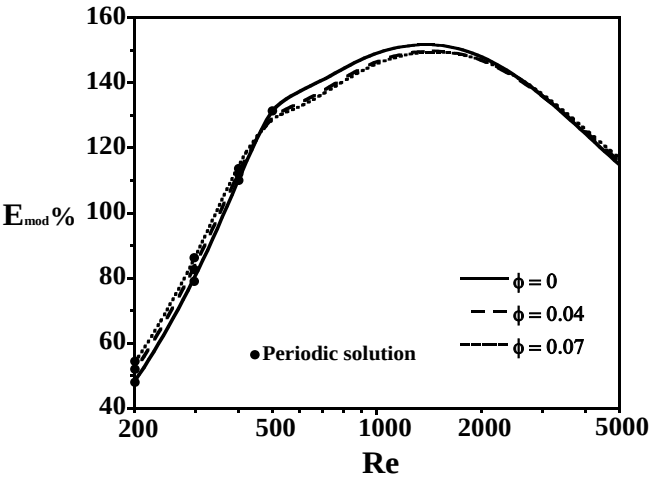

Fig. 8: Variations of the heat exchange improvement by ventilation mode, E_{mod}, with Re, and various values of ϕ

The heat-producing potential of the nanoparticles transfer improvement, for the two ventilation modes, is displayed in Figure 9 concerning variations with Re of the parameter $E_{nf} = [(Nu_{nf} - Nu_f) / Nu_f] \times 100$ for ϕ = 0.04 and 0.07. In the injection mode, E_{nf} increases monotonically through Re until a maximum amount is reached, obtained for Re_c = 600, which equals 6.5% / (9%) for ϕ = 0.04 / (0.07). Beyond Re_c, E_{nf} remains almost constant. For the suction mode, E_{nf} increases significantly with Re as long as the latter is greater than 1000. Below this value, E_{nf} is insensitive to any disturbance of Re. It is useful to mention that adding nanoparticles will make the suction mode more advantageous for improving heat exchange in comparison with the injection one for low and high Re. Also, it is noted that the difference in term of E_{nf}, resulting from the augmentation of ϕ from 0.04 to 0.07 keeps the same value for both modes and which is equal to 2.5%. However, for the injection case with Re < 500, this value is approximately 0.3%.

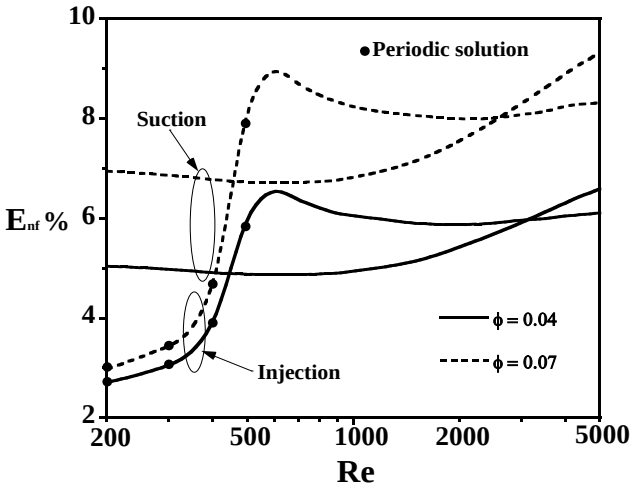

Fig. 9: Variations of the heat transfer improvement by nanoparticles addition, E_{nf}, with Re, for various values of ϕ in both modes

It is essential to give particular consideration to the assessment of the cavity's average temperature in such situations. Therefore, Figure 10 shows variations of this parameter relation to Re for the two ventilation cases and various values of ϕ. Specifically, in the injection case, raising Re to a critical number Re_c = 500 raises the average temperature $\overline{T}$, which strongly depends on ϕ. A constant Nu value in this Re region justifies this cavity reheating. (Figure 5 for the injection mode). Beyond Re_c, this tendency is reversed because the growing effect of Re is demonstrated by a drop of $\overline{T}$; this conduct is the result of the prevailing forced convection, which favors the evacuation of heat towards the exit and consequently assists in keeping the cavity cold. For the suction mode, the evolution of the average temperature $\overline{T}$ is distinguished by a notable reduction as Re increases. This is because of the higher heat exchange by convection with the rise in the flow velocity. Also, the positive impact of the insertion of nanoparticles on average temperature is observed. In addition, it is underlined to mention that the results of $\overline{T}$ obtained in the suction mode are lower than those obtained in the injection mode, the suction case effectively cools the cavity. For clarity, it should be mentioned that switching from the injection to the suction type results of $\overline{T}$ in the

reduction of almost 86% for Re = 1000 and $\phi = 0.04$.

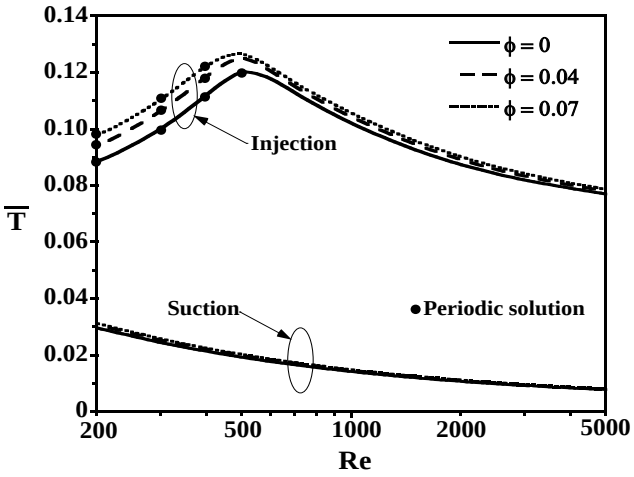

Fig. 10: Variations, of the mean temperature, $\overline{T}$, with Re, for different values of ϕ in both modes.

7 Conclusions

Nanofluid mixed convection in a multi-vented cavity heated from the bottom has been studied by taking injection and suction cases of forced external flows. Considering the results, the following conclusions have been drawn:

- ✓ Increasing the volume fraction of nanoparticles increases the rate of heat transmission for all values of Re in both modes; such behavior is weak for low values of Re in injection mode.
- ✓ The mean temperature is significantly raised with dispersed nanoparticles within the enclosure for the two modes of forced flow.
- ✓ A higher thermal efficiency is achieved in the suction mode by increasing heat transport across the cavity, with or without nanoparticles.
- ✓ Applying the suction mode usually results in improved cavity cooling because it reduces the average temperature values.

References:

[1] R. Y. Jou and S. C. Tzeng, Numerical research of nature convective heat transfer enhancement filled with nanofluids in rectangular enclosures, *International Communications in Heat and Mass Transfer*, Vol. 33, 2006, pp. 727-736.

[2] K. Kahveci, Buoyancy driven heat transfer of nanofluids in a tilted enclosure, *Journal of Heat Transfer*, Vol. 132, No 6, 2010, p. 062501.

[3] E. Abu-Nada, Z. Masoud, H. F. Oztop and A. Compo, Effect of nanofluid variable properties on natural convection in enclosures, *International Journal of Thermal Sciences*, Vol. 49, No 3, 2010, pp. 479-491.

[4] M. Corcione, Heat transfer features of buoyancy-driven nanofluids inside rectangular enclosures differentially heated at the sidewalls, International Journal of Thermal Sciences, Vol. 49, No 9, 2010, pp. 1536-1546.

[5] M. Corcione, Empirical correlating equations for predicting the effective thermal conductivity and dynamic viscosity of nanofluids, *Energy Conversion and Management*, Vol. 52, No 1, 2011, pp. 789-793.

[6] F. H. Lai and Y. T. Yang, Lattice Boltzmann simulation of natural convection heat transfer of Al_2O_3/water nanofluids in a square enclosure, *International Journal of Thermal Sciences*, Vol. 50, No 10, 2011, pp. 1930-1941.

[7] M. Bouhalleb and H. Abbassi, Numerical investigation of heat transfer by CuO-water nanofluid in rectangular enclosures, *Heat Transfer Engineering*, Vol. 37, No 1, 2016, pp. 13-23.

[8] A. A. Abbasian Arani, M. Mahmoodi and S. M. Sebdani, On the cooling process of nanofluid in a square enclosure with linear temperature distribution on left wall, Journal of Applied Fluid Mechanics, Vol. 7, No. 4, 2014, pp. 591-601.

[9] G. Wang, X. Meng, M. Zeng, H. Ozoe and Q. W. Wang, Natural convection heat transfer of copper-water nanofluid in a square cavity with time-periodic boundary temperature, *Heat Transfer Engineering*, Vol. 35, 2014, pp. 630-640.

[10] A. H. Mahmoudi, M. Shahi, A. H. Raouf and A. Ghasemian, Numerical study of natural convection cooling of horizontal heat source mounted in a square cavity filled with nanofluid, International Communications in *Heat and Mass Transfer*, Vol. 37, 2010, pp. 1135-1141.

[11] F. Garoosi, G. Bagheri and F. Talebi, Numerical simulation of natural convection of nanofluids in a square cavity with several pairs of heaters and coolers (HACs) inside, *International Journal of Heat and Mass Transfer*, Vol. 67, 2013, pp. 362-376.

[12] C. J. Ho, L. C. Wei and Z. W. Li, An experimental investigation of forced

convective cooling performance of a microchannel heat sink with Al_2O_3/water nanofluid, *Applied Thermal Engineering*, Vol. 30, No 2, 2010, pp. 96-103.

[13] S. M. H. Hashemi, S. A. Fazeli, H. Zirakzadeh and M. Ashjaee, Study of heat transfer enhancement in a nanofluid-cooled miniature heat sink, *International Communications in Heat and Mass Transfer*, Vol. 39, No 6, 2012, pp. 877-884.

[14] S. A. Fazeli, S. M. H. Hashemi, H. Zirakzadeh and M. Ashjaee, Experimental and numerical investigation of heat transfer in a miniature heat sink utilizing silica nanofluid, *Superlattices and Microstructures*, Vol. 51, No 2, 2012, pp. 247-264.

[15] H. Zirakzadeh, A. Mashayekh, H. N. Bidgoli and M. Ashjaee, Experimental investigation of heat transfer in a novel heat sink by means of alumina nanofluids, *Heat Transfer Research*, Vol. 43, No 8, 2012, pp. 709-720.

[16] F. Talebi, A. H. Mahmoudi and M. Shahi, Numerical study of mixed convection flows in a square lid-driven cavity utilizing nanofluid, *International Communications in Heat and Mass Transfer*, Vol. 37, No 1, 2010, pp. 79-90.

[17] F. Garoosi, S. Garoosi and K. Hooman, Numerical simulation of natural convection and mixed convection of the nanofluid in a square cavity using Buongiorno model, *Powder Technology*, Vol. 268, 2014, pp. 279-292.

[18] S. M. Sebdani, M. Mahmoodi and S. M. Hashemi, Effect of nanofluid variable properties on mixed convection in a square cavity, *International Journal of Thermal Sciences*, Vol. 52, 2012, pp. 112-126.

[19] A. A. Abbasian Arani, S. M. Sebdani, M. Mahmoodi, A. Ardeshiri and M. Aliakbari, Numerical study of mixed convection flow in a lid-driven cavity with sinusoidal heating on sidewalls using nanofluid, *Superlattices and Microstructures*, Vol. 51, No 6, 2012, pp. 893-911.

[20] M. Kalteh, K. Javaherdeh and T. Azarbarzin, Numerical solution of nanofluid mixed convection heat transfer in a lid-driven square cavity with a triangular heat source, *Powder Technology*, Vol. 253, 2014, pp. 780-788.

[21] M. Shahi, A. H. Mahmoudi and F. Talebi, Numerical study of mixed convective cooling in a square cavity ventilated and partially heated from the below utilizing nanofluid, *International Communications in Heat and Mass Transfer*, Vol. 37, No 2, 2010, pp. 201-213.

[22] A. H. Mahmoudi, M. Shahi and F. Talebi, "Effect of inlet and outlet location on the mixed convective cooling inside the ventilated cavity subjected to an external nanofluid", International Communications in Heat and Mass Transfer, Vol. 37, No 8, 2010, pp. 1158-1173.

[23] A. H. Mahmoudi and K. Hooman, Effect of a discrete heat source location on entropy generation in mixed convective cooling of a nanofluid inside the ventilated cavity, *International Journal of Exergy*, Vol. 13, 2013, pp. 299-319.

[24] E. Sourtiji, M. Gorji-Bandpy, D. D. Ganji and S. F. Hosseinizadeh, Numerical analysis of mixed convection heat transfer of Al2O3-water nanofluid in a ventilated cavity considering different positions of the outlet port, *Powder Technology*, Vol. 262, 2014, pp. 71-81.

[25] A. A. Mehrizi, M. Farhadi, H. H. Afroozi, K. Sedighi and A. A. R. Darz, Mixed convection heat transfer in a ventilated cavity with hot obstacle: effect of nanofluid and outlet port location, *International Communications in Heat and Mass Transfer*, Vol. 39, 2012, pp. 1000-1008.

[26] M. H. Esfe, S. Niazi, S. S. M. Esforjani and M. Akbari, Mixed convection flow and heat transfer in a ventilated inclined cavity containing hot obstacles subjected to a nanofluid, *Heat Transfer Research*, Vol. 45, No 4, 2014, pp. 309-338.

[27] I. Arroub, A. Bahlaoui, A. Raji, M. Hasnaoui and M. Naïmi, Cooling Enhancement by Nanofluid Mixed Convection inside a Horizontal Vented Cavity Submitted to Sinusoidal Heating, *Engineering Computations*, Vol. 35, No. 4, 2018, pp. 1747-1773.

[28] I. Arroub, A. Bahlaoui, S. Belhouideg, A. Raji and M. Hasnaoui, Numerical Investigation of Mixed Convection in a Tilted Multi-Vented Cavity Filled with Nanofluid Considering Different Positions of the Outlet Port, *AIP Conference Proceedings*, Vol. 2761, No. 1, 2023, p. 040027.

[29] A.S. Rikani, Numerical analysis of free heat transfer properties of flat panel solar collectors with different geometries, *Journal of Research in Science, Engineering and*

Technology, Vol. 9, No. 01, 2021, pp. 95-116.

[30] M Sultan, S., Tso, C. P., & M N, E. E. (2020). A case study on effect of inclination angle on performance of photovoltaic solar thermal collector in forced fluid mode, *Renewable Energy Research and Applications*, Vol. 1, No. 2, 2020,pp 187-196.

[31] N. A. Qasem, A. Abderrahmane, S. Ahmed, O. Younis, K. Guedri, Z. Said, A. Mourad, Effect of a rotating cylinder on convective flow, heat and entropy production of a 3D wavy enclosure filled by a phase change material, *Applied Thermal Engineering*, Vol. 214, 2022, p. 118818.

[32] M. M. Bhatti, A. Riaz, L. Zhang, S. M. Sait, R. Ellahi, Biologically inspired thermal transport on the rheology of Williamson hydromagnetic nanofluid flow with convection: An entropy analysis, *Journal of Thermal Analysis and Calorimetry*, Vol. 144, 2021, pp. 2187-2202.

[33] F. P. Incropera and D. P. DeWitt, *Introduction to Heat Transfer*, Wiley New York, 2002.

[34] I. Arroub, A. Bahlaoui, A. Raji, M. Hasnaoui and M. Naïmi, Varying Heating Effect on Mixed Convection of Nanofluids in a Vented Horizontal Cavity with Injection or Suction, *Heat Transfer Engineering*, Vol. 40, No. 11, 2019, pp. 941-958.

[35] M. Corcione, M. Cianfrini and A. Quintino, Two-phase mixture modeling of natural convection of nanofluids with temperature-dependent properties, *International Journal of Thermal Sciences*, Vol. 71, 2013, pp. 182-195.

[36] M. Corcione, M. Cianfrini and A. Quintino, Enhanced natural convection heat transfer of nanofluids in enclosures with two adjacent walls heated and the two opposite walls cooled, *International Journal of Heat and Mass Transfer*, Vol. 88, 2015, pp. 902-913.

[37] L. C. Woods, A note on the numerical solution of fourth order differential equations, *Aeronautical Quarterly*, Vol. 5, No 4, 1954, pp. 176-184.

[38] I. Arroub, A. Bahlaoui, S. Belhouideg, A. Raji and M. Hasnaoui, Combined effects of inclination angle and imposed flow on mixed convective cooling inside a vented cavity crossed by nanofluids, *Physical Chemistry Research*, Vol. 11, No.3, 2023, pp. 631-642.

[39] C. J. Ho, W. K. Liu, Y. S. Chang and C. C. Lin, Natural convection heat transfer of alumina-water nanofluid in vertical square enclosures: An experimental study, *International Journal of Thermal Sciences*, Vol. 49, 2010, pp. 1345-1353.

[40] T. B. Lennie, D. P. McKenzie, D. R. Moore and N. O. Weiss, The breakdown of steady convection, Journal of Fluid Mechanics, Vol. 188, 1988, pp. 47-85.

Contribution of Individual Authors to the Creation of a Scientific Article (Ghostwriting Policy)

The authors equally contributed to the present research, at all stages from the formulation of the problem to the final findings and solution.

Sources of Funding for Research Presented in a Scientific Article or Scientific Article Itself

No funding was received for conducting this study.

Conflict of Interest

The authors have no conflicts of interest to declare that are relevant to the content of this article.